SECTION 3. EARLY-FLIGHT STUDY: METHODS, STATUS, AND FRONTIERS

Chapter 10
Methods of Studying Early Theropod Flight

MICHAEL PITTMAN,[1] ASHLEY M. HEERS,[2] FRANCISCO J. SERRANO,[3] DANIEL J. FIELD,[4] MICHAEL B. HABIB,[5] T. ALEXANDER DECECCHI,[6] THOMAS G. KAYE,[7] AND HANS C.E. LARSSON[8]

ABSTRACT

The study of early theropod flight involves avialans as well as other pennaraptorans. It requires the study of anatomy that is familiar to the modern ornithologist, but also very different and alien. Early theropod flight therefore necessitates study methods that can incorporate what we know about sophisticated powered and unpowered flight in living birds while being mindful of the differences between them and the earliest theropod flyers. In this chapter we will survey key methods and approaches, covering their best-practice applications along the timeline of early theropod flight evolution and priorities for future method development.

INTRODUCTION

Locomotion plays a central role in the lives of most vertebrates, and reconstructing locomotor behaviors of extinct taxa is key to understanding some major evolutionary transitions—for example, the origin of walking tetrapods or swimming whales. But how do we reconstruct locomotion in extinct taxa when it is very difficult to compare them to modern forms?

When trying to decipher early theropod flight, researchers are faced with substantial anatomical differences between modern flying birds like pigeons and early birds like *Archaeopteryx* as well as their closely related nonavialan relatives. In particular, extant volant birds have a large keel on the sternum, which anchors two main flight muscles, the pectoralis for downstroke and the supracoracoideus for upstroke (George and Berger, 1966). Though the supracoracoideus is in a ventral position, it is

[1] Vertebrate Palaeontology Laboratory, Division of Earth and Planetary Science, the University of Hong Kong, Hong Kong.
[2] College of Natural and Social Sciences, California State University, Los Angeles.
[3] Dinosaur Institute, Natural History Museum of Los Angeles County, Los Angeles; and Real Academia Ciencias Exactas, Físicas y Naturales, Madrid.
[4] Department of Earth Sciences, University of Cambridge, Cambridge.
[5] Dinosaur Institute, Natural History Museum of Los Angeles County, Los Angeles.
[6] Division of Natural Sciences, Mount Marty College, Yankton, SD.
[7] Foundation for Scientific Advancement, Sierra Vista, AZ.
[8] Redpath Museum, McGill University, Montreal.

able to elevate and supinate (Poore et al., 1997a; Tobalske and Biewener, 2008) the wing because it loops through a donut-shaped triosseal canal and attaches to the dorsal surface of the humerus, similar to a pulley. *Archaeopteryx*, in contrast, has no triosseal canal and no ossified sternum, but some early avialans and possibly volant nonavialan pennaraptorans have either feature or both in an incipient form (Zhou and Zhang, 2002; Xu et al., 2003; Baier et al., 2007; Dyke et al., 2013; Zheng et al., 2014; Pei et al., in press). Consequently, at least some of the flight muscles of many early avialans and suspected volant nonavialan pennaraptorans were probably not very large, and would have had different configurations compared with extant birds. What does that mean in terms of the locomotor capacity of early birds and some nonavialan pennaraptorans?

The study of early theropod flight engages tailored methodologies with their own emphases to address the spectrum of form-function differences along the line of descent from the first theropod flyers to modern living ones. Theropod aerial locomotion seems to have multiple origins, the study of which involves anatomy that is very different to modern birds. At the other end of the theropod flight timeline, the origin of avian flight involves looking at a much more refined set of flight-related avian features that allowed birds to adopt different flight styles, but not the sophisticated powered flight of living birds. In this chapter we will survey key methods and approaches adopted in studying early theropod flight, detailing their best practice applications to the facets of this iconic field of pennaraptoran paleontology.

FORM-FUNCTION RELATIONSHIPS

Substantial efforts to characterize the morphology of early pennaraptoran theropods and investigate their relationship with flight function continue to greatly advance our knowledge of early theropod flight. This ranges from numerous studies assessing the functional morphology of single taxa (Navalón et al., 2015; Xu et al., 2015; Wang et al., 2017) to work focusing on one or a few anatomical features, such as feathers and/or wings (e.g., Burgers and Chiappe, 1999; Nudds and Dyke, 2010; Chiappe et al. 2019), tails (e.g., Gatesy and Dial, 1996; Gatesy, 2001; Pittman et al., 2013), the shoulder (e.g., Jenkins, 1993; Baier et al., 2007; Navalón et al., 2018), or the supracoracoideus muscle (e.g., Poore et al., 1997b). Recent efforts to leverage the locomotor variation among nearly 11,000 living species (Prum et al., 2015; Gill and Donsker, 2017) using large-scale datasets to characterize aspects of the avian flight apparatus have begun to bear fruit. New analytical techniques are showing that yet more high-fidelity flight-related soft-tissue details are hidden in the very best preserved pennaraptorans, especially those from China (Falk et al., 2016; Wang et al., 2017; see Serrano et al., chap. 13). Advancements in early flight studies have greatly benefited from the evolutionary context provided by a range of detailed phylogenetic analyses, the details of which are provided by Pittman et al. in chapter 2.

Large-scale Avian Anatomical Datasets: Seminal datasets like those by Greenewalt (1975) or Hartman (1961) have been extremely helpful in informing our understanding of early theropod flight (e.g., Dececchi et al., 2016; Pei et al., in press), but their use has generally fallen out of favor in recent times. The reason for this may be that these datasets are often created from amalgamations of other datasets or sources, so that specific specimens are rarely scored for all relevant measurements (Hartman, 1961; Greenewalt, 1975). A new generation of studies has begun to broach this data gap to quantify anatomical variation for key modules of the flight apparatus by using large comparative samples that draw on the majority of avian higher-order subclades. These studies have begun to yield form-function relationships that may provide new lines of investigation into early flight. This includes work on the furcula (Close and Rayfield, 2012) as well as on flight feathers (Feo et al., 2015) and skeletal proportions (Field et al., 2013; Serrano et al., 2015).

Feathers are among the most characteristic avian specializations, but quantitative compari-

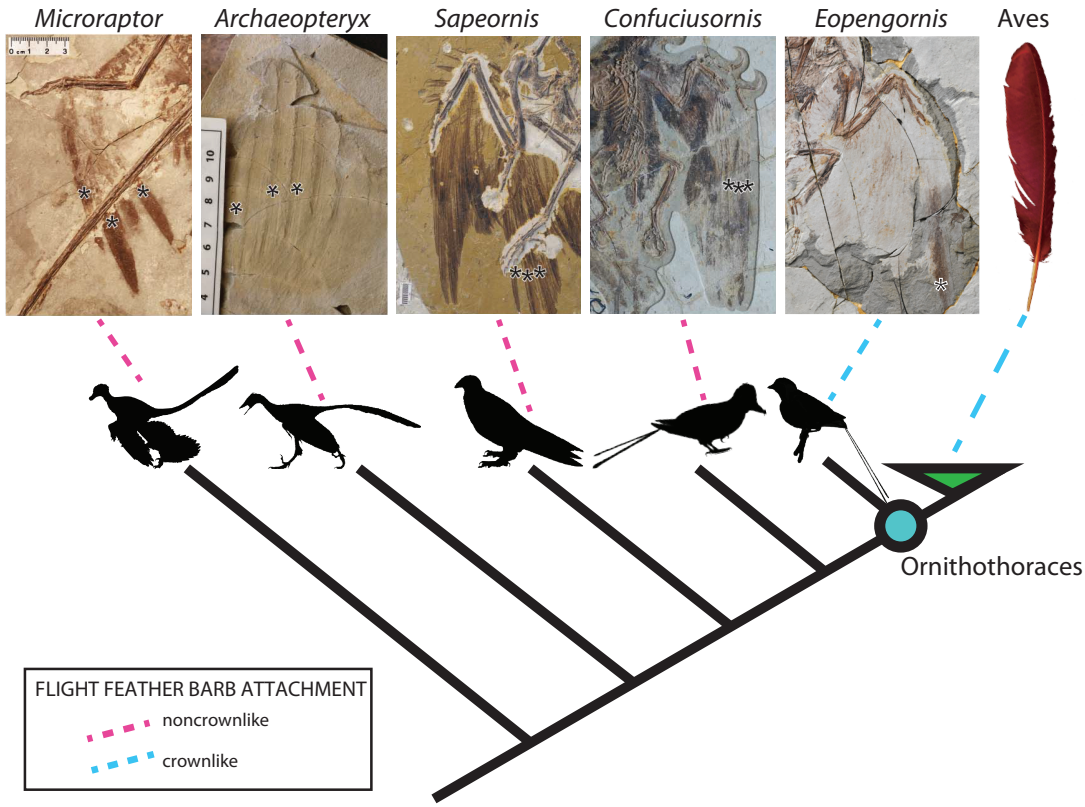

FIG. 1. Flight feather morphology across paravian phylogeny (modified from Feo et al., 2015). Early-diverging taxa (indicated by dashed pink lines) exhibit flight feather trailing edges characterized by narrow angles of barb-to-rachis attachment. The crownlike condition (broad angles of barb-to-rachis trailing edge attachment; blue dashed lines) arose on the internode subtending Ornithothoraces, and may have conferred a more flexible trailing edge of the wing during flight in order to increase feather-to-feather contact and maintenance of a coherent wing surface in flight during active downstrokes. Silhouettes from phylopic.org.

sons between flight-feather morphology in living and extinct total-clade birds are hampered by the rarity of intact fossil feathers and the preservation difficulty posed by their flexible feather vanes. A large comparative dataset examining feather-barb geometry was successfully generated and used to characterize macroevolutionary patterns in barb arrangement across the crown bird tree of life (Feo et al., 2015). Among other observations, this study observed that crown birds exhibit characteristic barb-to-rachis attachment angles on the leading and trailing edges of flight feathers (Feo et al., 2015). Primary feather barbs on a wing's leading edge that cut into the air during flight connect to the rachis at narrow attachment angles, providing a relatively inflexible airfoil for stability during flight, whereas barbs on the trailing edge of flight feathers connect to the rachis at broad angles of attachment, providing a more flexible vane in order to maintain a coherent wing surface through feather-to-feather contact. These patterns are generally conserved across crown birds. In contrast to this pattern, deinonychosaurians, like *Microraptor*, and early-diverging volant avialans, like *Archaeopteryx*, *Confuciusornis*, and *Sapeornis*, exhibit trailing edge barbs with angles of attachment indistinguishable from the narrow angles of

attachment of leading-edge barbs (fig. 1), suggesting that the trailing-edge vane flexibility—and associated benefits for maintaining a coherent trailing edge of the wing during flight—did not exist in these taxa (Feo et al., 2015). By contrast, more crownward avialans (e.g., Enantiornithes) appear to have exhibited the crown-like trailing-edge condition, suggesting that broad angles of trailing-edge barb-to-rachis attachment arose on the internode-subtending Ornithothoraces and were inherited by the ancestors of crown birds (fig. 1). This work suggests that despite an early origin of flight-feather asymmetry (Feduccia and Tordoff, 1979), "modern" flight feathers arose at a later-diverging point in paravian evolutionary history than previously recognized. Other aspects of feather morphology, such as emargination and its ability to offset the cost of slow flight also appear to have been later developments in avian evolution (van Oorschot et al., 2017), further stressing how the feathers of extant taxa are not identical to those of the earliest avialans.

Body mass is one of the most critical parameters in flight studies (Norberg, 2002; Videler, 2005; Pennycuick, 2008; Tennekes, 2009). In light of differing body mass estimates, inferences of a particular fossil taxon's flight potential could differ radically. The dependence of functional inferences on body mass places a premium on the attainment of accurate and precise estimates of fossil body size in paravians. Recent work aimed at improving methods for paravian body size estimation has focused on the development of multivariate and bivariate equations for body size estimation based on avian skeletal proportions (Field et al., 2013; Serrano et al., 2015). In addition to providing scaling equations for the estimation of mean body size in crown birds and nonavian avialans from skeletal measurements, these studies represent the first avian skeletal studies to explicitly provide equations for 95% prediction intervals on body mass estimates, providing better-informed constraints on uncertainty in fossil avialan body size estimates and their resulting functional hypotheses (fig. 2). Used with caution, these constraints can potentially have comparable benefits in more morphologically disparate nonavialan paravians. An encouraging development to emerge from such scaling studies is that relatively robust estimates of body mass can be reconstructed from the mostly fragmentary, isolated elements typically preserved in the avialan fossil record (fig. 2) (Louchart et al., 2009; Longrich et al., 2011; Brocklehurst et al., 2012; Field, 2017). Of 13 skeletal measurements investigated, 11 yielded especially high correlations with body size (R^2 >0.9). Moreover, scaling equations for several elements (e.g., femur length; fig. 3) scale uniformly for both flying and flightless extant birds, suggesting that these measurements are particularly appropriate for estimating body size in extinct taxa for which flying potential is uncertain (e.g., nonavian avialans). However, it is important to be mindful of how anatomical differences between extant and extinct taxa may affect results. Beyond the obvious relationship between body mass and flying potential, body mass is strongly associated with a host of important physiological, ecological, and biomechanical parameters (Schmidt-Nielsen, 1984; Rayner, 1988; Pollock and Shadwick, 1994; Brown, 1995; Ahlborn, 2000; Gillooly et al., 2001; Gillooly et al., 2002; Campione and Evans, 2012; Smith, 2012; Berv and Field, 2018), parameters that underscore the importance of robustly estimating body size in paleobiological studies of extinct fossil taxa.

Hidden flight-Informative Fossilized Soft Tissue Data: Newly available analytical techniques in modern paleontology have enabled more attention to be given to the discovery of fossil soft tissues, including soft tissues directly related to flight capability and performance. The feather impressions found in *Archaeopteryx* was the key evidence used to suggest that early birds were flight capable (Wellnhofer, 2009). Raking light for *Archaeopteryx* feather impressions has now given way to direct microscopic analysis of feathers, such as the Chinese feathered dinosaurs. Barbs are easily visualized with white light but

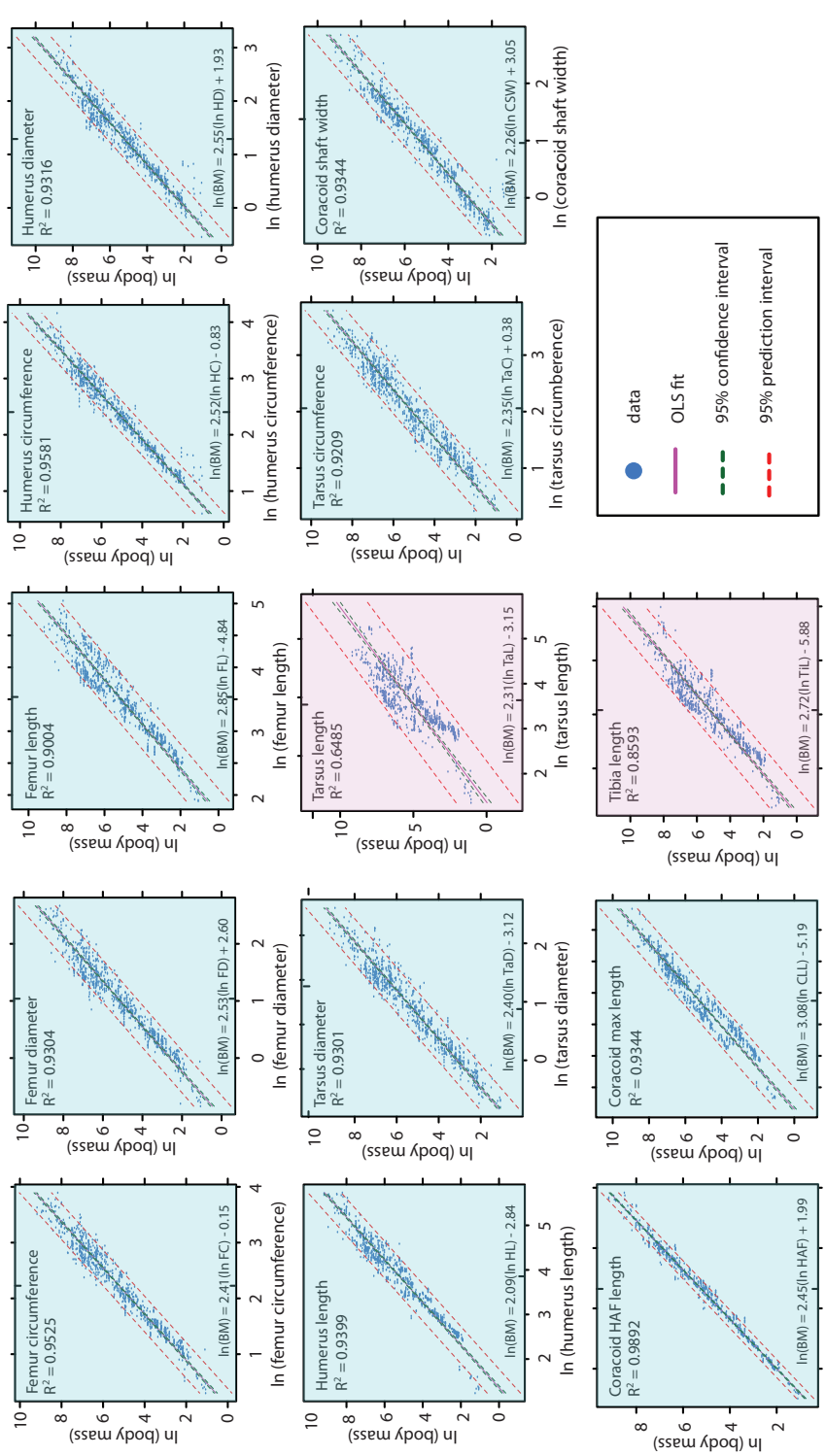

FIG. 2. Bivariate scaling equations for crown birds for 13 skeletal measurements, including 95% prediction intervals (modified from Field et al., 2013). Equations with $R^2 > 0.9$ are highlighted in blue; equations with $R^2 < 0.9$ are highlighted in pink.

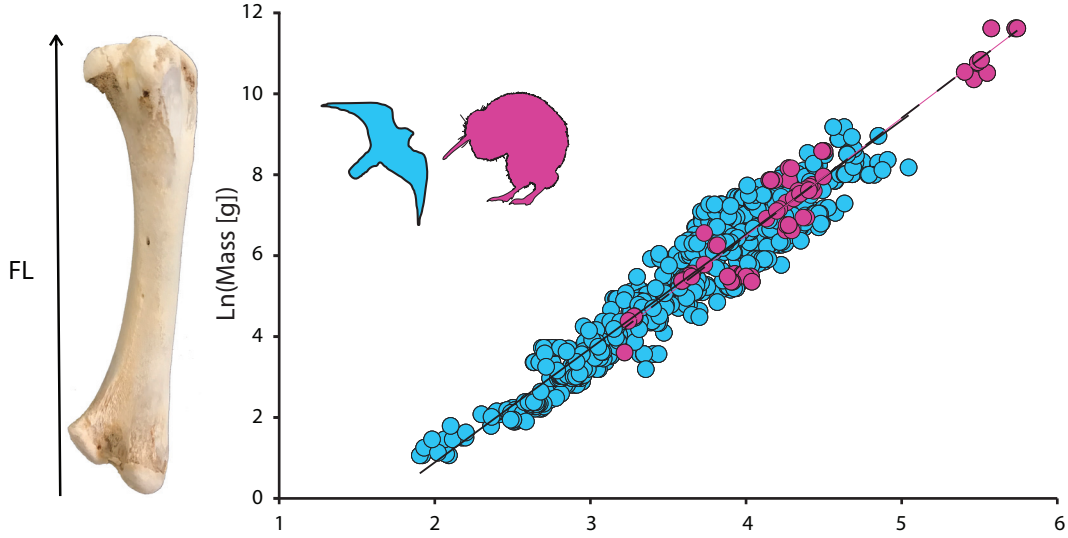

FIG. 3. Example of a bivariate scaling equation for femur length (D.J. Field, unpublished data) illustrating virtually invariant scaling equations for flying (blue) and flightless (pink) extant bird taxa. Datasets such as this will be useful for estimating live body mass for extinct avialans with unknown flying potential.

laser-stimulated fluorescence (LSF) is now capable of bringing out barbule structure by fluorescing sediment matrix to backlight nonfluorescent carbon films comprising fossil feathers (Kaye et al., 2015, 2019; Wang et al., 2017; to a lesser extent under UV: Hone et al., 2010). This application of LSF has important potential in reappraising known fossil feather diversity (Lefèvre, 2020; Xu 2020) and testing ideas of the evolution of feather rigidity and integrity that directly impact reconstructions of early flight. Neutron imaging also has the potential to contribute meaningful new data in the study of fossil feathers. While synchrotron elemental analysis has trouble with atomic numbers below silicon (Brown and Waychunas, 2004), neutrons work best on carbon and other lower atomic number elements. This makes it a unique elemental technique compared to alternatives for imaging soft tissues.

The UV lamp has now advanced to high power near UV wavelength lasers capable of fluorescing virtually all minerals. This allows clarifying osteology (Tischlinger and Unwin, 2004; Foth et al., 2014; Rauhut et al., 2018) and has produced the first quantifiable body outline of the early-diverging paravian *Anchiornis* (Wang et al., 2017) (see Pittman et al., chapters 1 and 2). The latter study revealed the wing's leading edge shape as well as arrangement of the feathers from the leading to trailing edge, providing the refined direct data of wing span and lift (= wing) surface (Wang et al., 2017). In chapter 13 of this volume, Serrano et al. used direct nonfeather-based soft-tissue data to refine calculations of flight performance using mechanically informed morphospace analysis for the first time.

The increasingly common use of nondestructive imaging in the study of the mostly skeletal portions of fossil birds provides an opportunity to develop augmented imaging protocols that can visualize and document preserved soft tissues, even before preparation (sensu Abel et al., 2012. and Schilling et al., 2014). Alternative imaging approaches like neutron imaging and proven soft-tissue imaging methods like LSF all have a role to play in this area. However, new analytical techniques also have a role in further curating existing specimens, such as by clarifying the integrity of

suspect fossils. For example, the extent of prior repair work can be clarified using regular and synchrotron x-rays (Rowe et al., 2001; Cau et al., 2017) and fluorescence imaging like LSF and UV (Kaye et al., 2015; Eklund et al., 2018).

Theropod Early Flight Performance

In-depth functional morphology knowledge of many of the earliest flying theropods as well as evolutionary context afforded by an impressive legacy of phylogenetic analyses (see chapter 1) has provided the basis for efforts to estimate early theropod flight performance. Our knowledge of flight performance of early birds has dramatically increased in recent years, including the reconstruction of flight styles that we are familiar with today, such as thermal soaring (Serrano and Chiappe, 2017), as well as support for powered flight potential in a number of nonavialan theropod taxa (Pei et al., in press). Herein we cover three of the most powerful approaches available: mechanically informed morphospace analysis, first-principles-based modeling and interactive musculoskeletal modeling and simulation.

Mechanically Informed Morphospace Analysis: In the previous section, body mass (M_b) was mentioned as a key variable known to influence flight in living birds and this is also true of wing span (B) and lift (= wing) surface (S_L) (Norberg, 2002; Videler, 2005; Pennycuick, 2008; Tennekes, 2009). Using a conservative approach that recognizes the statistical, phylogenetic, ecological, and taphonomic sources of error associated with early bird fossils, these key flight variables can be used to infer flight performance in early birds. By carefully selecting forelimb and hind-limb measurements for each early-diverging taxon, multiple regressions can be obtained that minimize these sources of error as well as predictive error (Serrano et al., 2015, 2017). Reliable estimates of M_b, B, and S_L from this approach enable direct comparisons between early and modern birds in morphospaces that include these variables. Fine estimates of B and S_L can also be obtained from outline reconstruction in well-preserved feathered fossils (Wellnhofer, 2009; Chiappe et al., 2014).

Morphospaces relating M_b with B and/or the length of the deltopectoral crest of the humerus (DPC) allow the flapping pattern of early birds to be approximated (Serrano and Chiappe, 2017). For a given M_b and B, modern birds that fly with alternating flapping and gliding periods have shorter DPCs than birds with a stricter flapping pattern. Based on lever theory (Alexander, 2003), the latter birds have higher mechanical advantage for moving the wing faster—hence flapping it more frequently—than the former ones. This approach provided support for a flight pattern less dominated by wing flapping in the early-diverging pygostylian *Sapeornis* (Serrano and Chiappe, 2017). In a similar way, estimations showed that enantiornithines *Concornis* and *Eoalulavis* had short wings in relation to their body mass and DPC, suggesting that they flew strictly using flapping flight with no gliding phases in steady flight (Serrano et al., 2018). In such a study, a combined analysis of the three basic variables allowed bounding flight to be specifically inferred in *Concornis* and *Eoalulavis*.

Valuable information about flying behavior of extinct birds also can be obtained from the calculation of the wing loading (i.e., $WL = M_b/S_L$) and the aspect ratio ($AR = B^2/S_L$). While AR provides information relative to drag and thrust (Rayner, 1993; Swaddle and Lockwood, 2003; Meseguer and Sanz-Andres, 2007; Shyy et al., 2008), the WL provides information about the flight speed and turn radius (Von Mises, 1945; Norberg, 2002; Tennekes, 2009). In the case of *Sapeornis*, the relatively low AR of its wings indicated a continental (= thermal) soaring capacity instead of dynamic soaring (Serrano and Chiappe, 2017). In other cases, the low values of AR and WL estimated for *Junornis* and *Orienantius* suggested that these enantiornithines may have been capable of rapid takeoff and tight turns (Liu et al., 2017, 2019).

In many cases the aerial inferences obtained from morphospaces can be validated by constructing aerodynamic models based on the estimates of M_b, B, and S_L. Such models allow the

checking of the power margin during flapping flight and gliding patterns. This type of analysis supported conclusions that early birds like *Sapeornis* and *Gretcheniao* were incapable of generating sufficient power for sustaining prolonged flapping flight (Serrano and Chiappe, 2017; Chiappe et al. 2019), and also that *Concornis* and *Eoalulavis* could improve their efficiency of transport switching from continuous flapping to bounding (Serrano et al., 2018).

First-Principles-Based Modeling: These approaches to estimating flight performance rely on fundamental properties of aerodynamics and morphology that apply to all flying systems. They typically utilize a comparative framework, because calculations of exact performance values in fossil taxa are difficult to make with precision without a very large number of variables that are often not directly observable in fossils. The relative differences in performance, however, can often be robustly inferred using first principles approaches.

In the context of flight origins and evolution, modeling is often best approached from a dynamics perspective. Reconstructing kinematics with confidence requires a more species-specific approach, such as simulation or range-of-motion analysis from analogous living taxa (see Interactive Musculoskeletal Modeling and Simulation Method below). Typically, dynamics models must still make some kinematic assumptions. More conservative kinematic assumptions will yield more robust conclusions regarding dynamics. As an example, in our recent work on microraptorine flight dynamics (see Dececchi et al., chapter 11), we made only two kinematic assumptions: (1) the hind limbs generated the launch prior to the wing being engaged, (2) there was a sufficient range of motion to generate a viable flight stroke for climb out. For all taxa, we used only configurations in which the hind limbs (and therefore hind wings, where present) were held under the body in a vertical configuration. The first of these assumptions is conservative because the use of the stance limbs to engage takeoff is a universal trait of flying animals. The second assumption is conservative because it requires only that there be at least one motion set that provides sufficient wing amplitude for flight. This is therefore more conservative than specifying a particular flight stroke. Lift from the hindwings, in this configuration, potentially contributes to stability and control during flight, as the lift would be oriented laterally, rather than upward. It would not contribute to weight support or thrust, which we assume comes only from the forelimbs (and potentially the tail, but only for pitch authority).

Modeling approaches of this kind are particularly useful for determining those variables that have a particularly large effect on the performance outcome of interest. In the case of our microraptorine flight performance work, we found that maximal wing loading and specific lift capacity are strong criteria for evaluating flight performance in a comparative dataset of fossil taxa. These two criteria were devised from theoretical and in vivo work on extant avians and present easily testable benchmarks that accurately model the minimal thresholds needed to discern volant from flightless taxa (Meunier, 1951; Marden, 1987; Livezey, 1992; Guillemette and Ouellet, 2005)

For example, for taxa without complete primary feathers preserved, feather length was modeled on closely related taxa and wing area was calculated based on the methods presented in Dececchi et al. (2016). Geometric measurements were all taken using standard digital calipers. Wingspan was taken as 2.1× the summation of the lengths of the humerus, ulna and metacarpal II, and the longest distal primary (Dececchi et al., 2016). Wing chord was taken as 65% of the longest distal primary length (Dececchi et al., 2016). Wing loading is based on body weight estimated as per above (kg) over wing area (cm^2). Specific lift, here used as the lift force generated in the vertical plane is based on Marden's model (Marden, 1987). This model has been suggested to underestimate maximum vertical force produced (Buchwald and Dudley, 2010), thus these

values may represent a conservative estimate of force produced in these taxa. Specific lift = FMR × Po,m × (L/P) where FMR is the flight muscle ratio, which is assigned at a constant value of 10% of body weight across all taxa examined. This is at the lower range of the values seen in volant birds and is likely a significant overestimation for all nonparavian taxa based on recent 3D modeling work (Allen et al., 2013). The methods used here will help us to refine these estimates by producing more accurate body-outline reconstructions that place quantitative constraints on musculature. Po,m is the maximum muscle mass-specific power output based on values from extant birds. As Po,m is unknown for nonavialan theropods, three separate calculations were made that span the range of Po,m values that could have reasonably been expected (225, 250, and 287 Wkg^{-1}). However, we use the two extremes (225 and 287 Wkg^{-1}) to reconstruct minimum and maximum flying ability. We assume that all thrust is lift generated, and so the estimates of required power for flight essentially relate to the power that must be exerted against drag to generate sufficient lift for flight. Drag can contribute to thrust, but this is a relatively sophisticated dynamic, and lift-generated thrust dominates in living flying animals in the size range relevant to our study. The value of 225 Wkg^{-1} was suggested by Marden (1994) as the mean value for burst flight in birds. Work by Guillemette and Ouellet (2005) suggested that a range between 225 and 250 Wkg^{-1} more accurately mimics values seen in the Common Eider, a bird with short wings that displays some of the highest wing-loading values seen in extant birds, two features that resemble the condition seen in the extinct taxa examined here. The value of 287 Wkg^{-1} was based on the values calculated for Chukar partridges (Askew et al., 2001), a short burst flight taxon previously used as a model for early flight in theropods. Our work here will help refine these estimates and help us constrain these values even further. L/P is calculated from:

$$\log10\ (L/P) = -0.440 \log10 \text{ muscle mass} + 0.845 \log10 (\text{wingspan}/2) - 2.239$$

To improve optimization of the data we screened the coelurosaurians based on their presence of vaned feathers, which are integral to the production of aerodynamic forces; terminals for which feather condition is unknown were considered to have the same state as their ancestor, which is the condition predicted by our recent phylogenetic hypothesis (Pei et al., in press). If a taxon showed both wing-loading values below 2.5 gcm^{-2} (which has been estimated to be the upper limit for flight in extant birds: Meunier, 1951; Guillemette and Ouellet, 2005) as well as the potential to generate lift values more than 9.8 Nkg^{-1}, we suggest that this taxon has the potential to achieve takeoff and powered flight. We use linear parsimony to reconstruct wing loading and specific lift values over our tree topology. In this project we use the upper and lower limits recovered for *Microraptor* to see whether this affects the results of surrounding nodes, if at all. We will also consider tail area and shape, mostly for its role in determining the center of lift and providing pitch stability, adopting the approach previously utilized by one of the authors (MBH – see Han et al., 2015). In chapter 11, Dececchi et al. develop this approach further by presenting the first ontogenetic trajectory of flight and flapping-related behaviors in the nonavialan theropod *Microraptor*, which are directly compared to similar curves produced for extant birds (Heers and Dial, 2012).

Interactive Musculoskeletal Modeling and Simulation: This method has been widely used to study human locomotion, and adapted for use with extant animals such as chimpanzees (O'Neill et al., 2013) and extinct animals such as *Tyrannosaurus rex* (Hutchinson et al., 2005) and *Mussaurus* (Otero et al., 2017). Musculoskeletal modeling and simulation use programs like SIMM (Software for Interactive Musculoskeletal Modeling; Musculographics, Inc., http://www.musculographics.com/) and OpenSim (http://opensim.stanford.edu/) (Delp et al., 2007) to construct digital, musculoskeletal models and then simulate different behaviors to analyze muscle function or determine, for example, whether muscles would

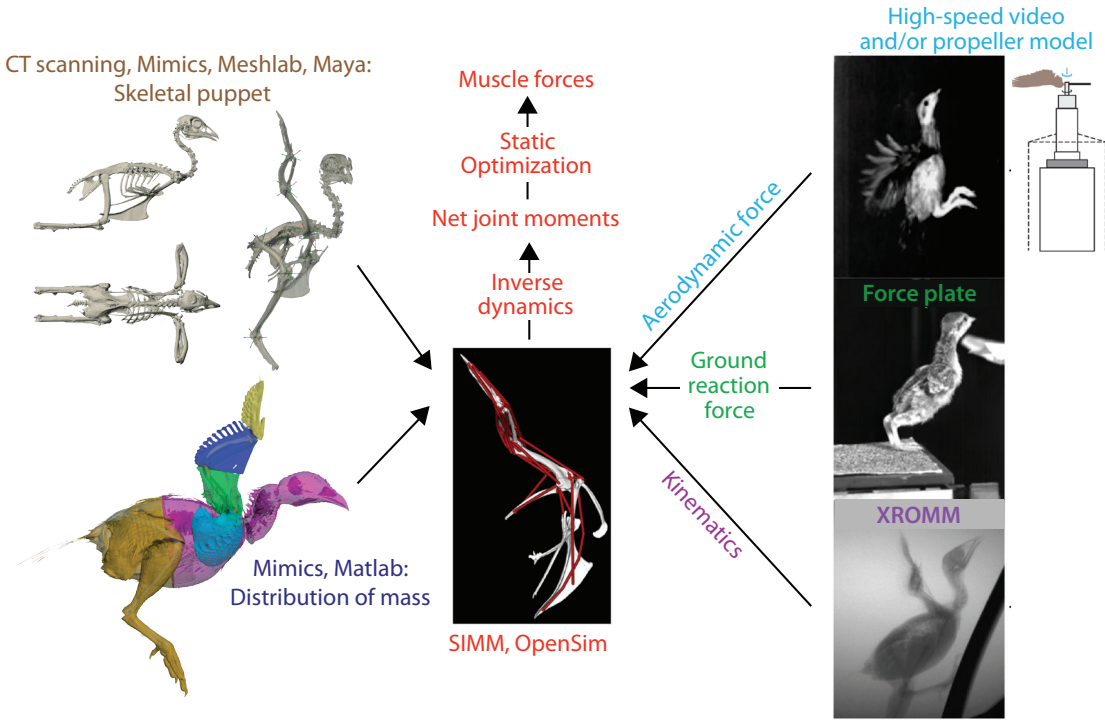

FIG. 4. Interactive musculoskeletal modeling and simulation involves 4 steps: (1) Computed tomography (CT) scanning, (2) dissection, (3) measurement of kinematics, and (4) measurement of all external forces. Modified from Heers, et al., 2016, 2018.

be strong enough to perform a particular behavior. For extant animals, musculoskeletal modeling involves four steps (fig. 4):

1. Computed Tomography Scanning: CT scanning of the animal in question, to construct a skeletal "puppet." This three-step process involves:

Isolating Skeletal Elements: Importing CT slices into programs such as Mimics (Materialise, Inc., Leuven, Belgium) or Osirix/Horos (Rosset et al., 2004), and using a density threshold to isolate skeletal elements (e.g., wing bones in a bird), which are then saved as three-dimensional objects (e.g., .obj files).

Constructing a Hierarchical Joint Coordinate System: This is often done by importing the skeletal elements into Maya (Autodesk; http://autodesk.com/) to align and link bones together through joints. A "zero" or resting position and coordinate systems for each joint must be defined. Joint-coordinate systems (Grood and Suntay, 1983) are typically defined anatomically, either based on the anatomy of the bones articulating at the joint or based on the morphology of the joint itself, though they can also be defined kinematically (i.e., joint location and axes of rotation can be calculated based on how bones are translated and rotated about each other during locomotion).

Determining Mass Distribution: Once the skeletal "puppet" is constructed, the distribution of mass must be quantified for each moveable body segment. Mimics, for example, can be used to digitally segment the animal into hind limb, trunk, brachial, antebrachial, and manual segments, depending on the animal and behavior in question. Each segment includes all tissues associated with that segment (bones, muscles, skin, fat, etc.). Assuming a tissue density of 1060 kgm^{-3}, a custom script (Allen et al. 2013) can then calculate the mass,

centre of mass, and inertial tensor for each body segment, based on its volume. These values determine the inertial properties of each moveable segment.

2. Dissection: This is done to add representations of muscles to the skeletal model. Model muscles, added in SIMM, are specified by:

Muscle Geometry: Origin(s), insertion(s), and path(s) between them. "Via points" or "wrapping objects" can be added to prevent the muscle from passing through bone.

Muscle Architecture: Optimal fibre length (typically taken as the length of muscle fascicles at rest: Zajac, 1989) and average pennation angle, which are important determinants of muscle strain (changes in length) and stress (force per unit physiological cross-sectional area).

Maximum Isometric Muscle Force: This is calculated from the physiological cross-sectional area of the muscle (area perpendicular to muscle fibres).

Tendon Slack Length: This is the length beyond which a muscle's tendons begin resisting stretch and producing force; this essentially specifies how much force is produced actively, by muscle fibers contracting, versus passively, by tendon(s) being stretched. Tendon slack length is calculated using an algorithm (Manal and Buchanan, 2004) that analyzes the shortening and lengthening behavior of muscle-tendon units over a large range of motion.

For more complex (dynamic) simulations, physiological properties such as maximal contractile velocity, force-velocity relationships, and activation-deactivation dynamics are included as well.

3. Measurement of Joint Kinematics: For some animals and behaviors, this is accomplished with high-speed visible light video. For birds and/or behaviors involving rapid movement, this may require X-ray Reconstruction of Moving Morphology (www.xromm.org).

4. Measurement of All External Forces Acting on the Animal: In addition to gravity, this may include ground reaction, aerodynamic, and/or hydrodynamic forces. Ground reaction forces are recorded by force plates, whereas fluid dynamic forces may be calculated using techniques like PIV (particle image velocimetry) (Tobalske and Dial, 2007) and "propeller models" (Heers et al., 2011; Dial et al., 2012), or measured using newly developed Aerodynamic Force Platforms (Lentink et al., 2015). For each force, a magnitude, direction, and location must be provided. Magnitude, direction, and sometimes location vary through a stroke or stride cycle.

In short, steps 1 and 2 result in the construction of an anatomical (musculoskeletal) model, and steps 3 and 4 involve collecting kinematic and kinetic data, which are required for simulation. Once a musculoskeletal model is constructed and the necessary experimental data are collected, various types of simulations can be performed in OpenSim:

Muscle Moment Arms: At the most basic level, the musculoskeletal model and joint kinematics can be used to calculate muscle moment arms through a stroke or stride cycle. The moment arm of a muscle indicates (a) what action it would perform if it were activated, and (b) how effective it would be at performing that action, because a muscle's ability to transform force into bone movement depends both on muscle force (which is proportional to muscle size) and the length of the muscle's moment arm. Thus, musculoskeletal models are useful tools for predicting muscle function(s).

Static Simulations: These take simulations one step further by calculating the timing and level of muscle activations during the movement of interest. First, *inverse dynamics* uses the musculoskeletal model, kinematics, and external loads provided to calculate the net joint moments that would be required to produce the simulated motion. A *static optimization* routine then resolves the net moments into individual muscle moments (muscle force times muscle moment arm) at each time step by minimizing the sum of squared muscle activations. This type of simulation can be used for a variety of purposes—for example, to compare simulated muscle activations with activations recorded in vivo

and thereby validate a model, to more explicitly determine muscle function (which depends not only on muscle moment arms, but also on muscle activation and joint kinematics), or to determine whether the modeled muscles are strong enough to drive various behaviors. One disadvantage of static simulations is that they consider each time step independently, and cannot account for time-dependent physiological properties such as force-velocity relationships or activation-deactivation dynamics. At this point in time, OpenSim's static optimization routine also assumes that tendons are rigid, and thus does not account for the storage and release of elastic energy. These two limitations must be addressed for behaviors involving rapid limb movements, such as flapping or jumping (see Heers et al., 2018).

Dynamic Simulations: Unlike static simulations, dynamic simulations account for time-dependent properties but require extensive knowledge of muscle physiology and can be difficult to work with. One type of dynamic simulation is forward dynamics. When muscle activations are known (e.g., previously measured using electromyography), they can be used to predict what type of locomotor behavior would result, given the animal's musculoskeletal anatomy and the muscle activations. Forward dynamics can thus be used to validate a model (does the behavior I'm trying to model actually occur with the given inputs?), and to compare or predict how muscle anatomy and activation affect locomotion (does locomotor behavior/performance differ because muscle anatomy and/or activations differ?).

Together, musculoskeletal modeling and simulation provide a dynamic, three-dimensional, whole-body perspective on locomotion in living animals, by analyzing how the skeleton, muscles, and feathers (which produce external, i.e., aerodynamic, forces) all work together during locomotion. Once a modeling and simulation approach has been worked out, additional questions that would be impossible to answer working solely with live animals can be explored. For example, anatomical features (e.g., bony processes, joint morphology, muscle size), as well as kinematic (i.e., the wing stroke) and/or kinetic (i.e., aerodynamic force production) properties can be altered to assess their effects on locomotion or muscle performance. Musculoskeletal modeling and simulation thus allow for a more explicit examination of form-function relationships, by allowing anatomical, kinematic, kinetic, and/or physiological features to be individually adjusted and their effects on locomotion determined. Consequently, this approach is also one of the most quantitative methods for reconstructing locomotion in extinct animals.

For extinct animals, modeling and simulation procedures are similar but require more assumptions. These assumptions must be analyzed through sensitivity analyses and validated by comparison with models of living homologs or analogs (Hutchinson, 2011). For example, step 1 requires assumptions about the distribution of mass and about joint anatomy, because the soft-tissue components of joints are usually not preserved. For step 2, although the geometry of some muscles can be reconstructed based on muscle scars and phylogenetic bracketing, muscle size, architecture, and physiology must always be extrapolated based on knowledge of living counterparts. Joint kinematics (step 3) and external forces (step 4) must also be inferred, potentially by phylogenetic bracketing coupled with analyses of joint range of motion and body size scaling. For all such inferences, it is probably best to analyze a range of possible anatomical, kinematic, and kinetic inputs (i.e., conduct a sensitivity analysis), which results in a range of "answers" to questions but reflects the uncertainty in these types of analyses and can highlight results that are robust to modeling or simulation assumptions. Regardless of how many models or simulations are considered, the modeling and simulation procedure must be validated by comparison with similar models and simulations of living animals. Locomotor capabilities are known in living animals, and the degree to which a musculoskeletal model and simulation can mimic those capabilities indicates our level of confidence in the modeling and simulation of locomotion in extinct animals.

Musculoskeletal modeling and simulation have been used to study posture and locomotor capacity (i.e., running speed) of theropods such as *Tyrannosaurus rex* (Hutchinson et al., 2005), and efforts are currently underway to apply this approach to the evolution of avian flight (Heers and Carney, 2017). For example, by simulating a range of potential flapping kinematics in key taxa like *Archaeopteryx* and in earlier and later diverging forms, we can assess which behaviors were potentially possible at different evolutionary stages and examine how evolutionary changes in morphology might have facilitated the origins of bird flight.

In summary, when used in conjunction with studies on live animals, musculoskeletal modeling and simulation are extremely useful tools for exploring how different anatomical features (bones, muscles, feathers) work together during locomotion. In addition, this technique allows anatomical, kinematic, and/or kinetic properties to be systematically adjusted to explicitly examine form-function relationships in ways that cannot be done empirically. Once a modeling and simulation approach has been tested using an extant analog or homolog, similar procedures can be applied to fossils to assess locomotor potential. Uncertainties in the musculoskeletal anatomy, kinematics, and kinetics of extinct animals are accounted for by using multiple models and simulations, resulting in a range of "answers" but highlighting results that are robust to modeling or simulation assumptions. Because of this, musculoskeletal modeling and simulation is one of the most rigorous tools available for assessing locomotor potential in extinct animals, including theropods with feathered forelimbs.

DISCUSSION

The methods surveyed here have all had significant impact on our understanding of early theropod flight and have been validated. This includes the example of first-principles-based modeling for the ultimate origins of theropod flight, which aligns with recent results of extremely detailed, single-species simulation approaches by a coauthor (A.M.H.) (Heers et al., 2018). Such validation is welcome and underscores the complementary nature of these two methods. For example, while musculoskeletal modeling and simulations offer a vital dynamic, three-dimensional, whole-body perspective, first-principles-based modeling is readily scalable and applicable to large, comparative datasets allowing it to identify macroevolution patterns and trends more easily (e.g., in chapter 11 by Dececchi et al.). Such a "prospect and then mine" relationship between these two methods is synergistic and should be further developed and coordinated moving forward.

Estimating flight performance requires significant time to set up, particularly musculoskeletal modeling and simulation, but their analytical products (i.e., spreadsheet equations, aerodynamics software, 3D interactive computer models) can often be reasonably easily modified if subsequent analyses involve similar subjects. In the case of mechanically informed morphospace analysis, functional morphology of structures (e.g., deltopectoral crest of the humerus) or other estimated variables (e.g., wing span and wing surface) can be compared with a large dataset of modern birds. Based on physics principles, this comparison has provided relevant information on the flight performance of a few early-diverging birds (Liu et al 2017, 2019; Serrano and Chiappe 2017; Serrano et al 2018; Chiappe et al. 2019). In addition, this approach can be complemented and validated through the construction of aerodynamic models of early birds using, for example, the software Flight v. 1.24 developed for modern birds (www.bio.bristol.ac.uk/people/pennycuick.htm; Pennycuick, 2008), which reduces the time needed to set up new analyses. The publication of several landmark studies in recent years (Dececchi et al., 2016; Heers et al., 2016; Serrano and Chiappe, 2017; Serrano et al., 2017; Heers et al., 2018; Serrano et al., 2018; Pei et al., in press) therefore promises a potentially rapid expansion in flight-performance studies in the not too distant future.

All methods of flight-performance estimation require assumptions with many needing parameters obtained from living birds because they are simply unknown in fossil taxa, e.g., the power output of flight muscle. However, with thousands of fossil birds available, it is understandable that specimens that might provide direct estimates of certain parameters may be overlooked. The leading-edge wing shape of the early-diverging paravians *Anchiornis* and *Microraptor*—as revealed by LSF (Wang et al., 2017; co-author MP & TGK, unpublished data)—are good examples of otherwise unknown information that directly affects estimations. In this case this information improves our estimation of wing area, which has since been considered in subsequent studies (Pei et al., in press), including in chapter 11 of this volume. Also in this volume, Serrano, et al. (chapter 13) use the lateral body outline of the early diverging avialan *Sapeornis*—as observed under LSF—to directly estimate the body's disc surface generating drag during flight (S_b). This surface and the body drag coefficient—which is better estimated knowing S_b—are influential parameters in modeling flight dynamics. New analytical techniques like LSF offer improved characterization of feathering, mass distribution, joint geometries, and other key modeling parameters, particularly contentious ones like feather structure as related to rigidity in flight, thereby increasing the accuracy of our understanding of early theropod flight. However, at least a portion of the missing data is probably available from existing specimens even using standard microscopy methods, such is the bounty of fossil specimens currently available. For example, some fossil taxa like *Confuciusornis* and *Anchiornis* are known from large sample sizes that are yet to be fully examined (Wang et al., 2017; Navalón et al., 2018) and the rate of new taxon discovery remains high (see Pittman et al., chapter 2). While it is easy to take this advice as a need to ramp up the number of specimens studied, past work and that by Serrano et al. (chapter 13) show that even a handful of feathered well-preserved specimens can provide accurate estimates (Liu et al., 2017; Serrano and Chiappe, 2017; Serrano et al., 2018). First-principles-based modeling remains the most readily adaptable method for studying flight performance across the breadth of Pennaraptora, but as better fossil data help to minimize potential sources of error in key parameters in particular (i.e., body mass, wing space, and lift surface), this situation could change and potentially present an opportunity for consensus results across multiple methods in the future.

ACKNOWLEDGMENTS

We would like to thank the attendees of the International Pennaraptoran Dinosaur Symposium and our reviewers for their comments and suggestions, which helped to improve the quality of this manuscript. The symposium was held at the University of Hong Kong and was supported by Kenneth HC Fung and First Initiative Foundation. This study was also supported by the Research Grant Council of Hong Kong's General Research Fund (17103315 to M.P.) and the RAE Improvement Fund of the Faculty of Science, the University of Hong Kong (to M.P. and T.G.K.). The participation of D.J.F. was also supported by UK Research and Innovation Future Leaders Fellowship MR/S032177/1.

REFERENCES

Abel, R.L., C.R. Laurini, and M. Richter. 2012. A palaeobiologist's guide to 'virtual' micro-CT preparation. Palaeontologica Electronica 15: 6T.

Ahlborn, B.K. 2000. Thermodynamic limits of body dimension of warm blooded animals. Journal of Non-Equilibrium Thermodynamics 25: 87–102.

Alexander, R.M. 2003. Principles of animal locomotion, Princeton: Princeton University Press.

Allen, V., K.T. Bates, Z.H. Li, and J.R. Hutchinson. 2013. Linking the evolution of body shape and locomotor biomechanics in bird-line archosaurs. Nature 497: 104–107.

Askew, G.N., R.L. Marsh, and C.P. Ellington. 2001. The mechanicalpower output of the flight muscles of Blue-breasted Quail (*Coturnix chinensis*) during take-off. Journal of Experimental Biology 204: 3601–3619.

Baier, D.B., S.M. Gatesy, and F.A. Jenkins. 2007. A critical ligamentous mechanism in the evolution of avian flight. Nature 445: 307–310.

Berv, J.S., and D.J. Field. 2018. Genomic Signature of an Avian Lilliput Effect across the K-Pg Extinction. Systematic Biology 67: 1–13.

Brocklehurst, N., P. Upchurch, P.D. Mannion, and J.M. O'Connor. 2012. The completeness of the fossil record of Mesozoic birds: implications for early avian evolution. PLoS One 7: e39056.

Brown, G.E., Jr., and G.A. Waychunas. 2004. X-ray absorption spectroscopy: introduction to experimental procedures. Stanford University, accessed 18/04/2018.

Brown, J.H. 1995. Macroecology, Chicago: University of Chicago Press.

Buchwald, R., and R. Dudley. 2010. Limits to vertical force and power production in bumblebees (Hymenoptera: *Bombus impatiens*). Journal of experimental Biology 213: 426–432.

Burgers, P., and L.M. Chiappe. 1999. The wing of *Archaeopteryx* as a primary thrust generator. Nature 399: 60–62.

Campione, N.E., and D.C. Evans. 2012. A universal scaling relationship between body mass and proximal limb bone dimensions in quadrupedal terrestrial tetrapods. BMC Biology 10.

Cau, A., et al. 2017. Synchrotron scanning reveals amphibious ecomorphology in a new clade of bird-like dinosaurs. Nature 552: 395–399.

Chiappe, L.M., et al. 2014. A new specimen of the Early Cretaceous bird *Hongshanornis longicresta*: insights into the aerodynamics and diet of a basal ornithuromorph. PeerJ 2: e234.

Chiappe, L.M., et al. 2019. New *Bohaiornis*-like bird from the Early Cretaceous of China: enantiornithine interrelationships and flight performance. PeerJ 7: e7846.

Close, R.A., and E.J. Rayfield. 2012. Functional morphometric analysis of the furcula in mesozoic birds. PLoS One 7(5): e36664.

Dececchi, T.A., H.C.E. Larsson, and M.B. Habib. 2016. The wings before the bird: an evaluation of flapping-based locomotory hypotheses in bird antecedents. PeerJ 4: e2159.

Delp, S.L., et al. 2007. OpenSim: open-source software to create and analyze dynamic simulations of movement. IEEE Transactions on Biomedical Engineering 54: 1940–1950.

Dial, T.R., A.M. Heers, and B.W. Tobalske. 2012. Ontogeny of aerodynamics in mallards: comparative performance and developmental implications. The Journal of Experimental Biology 215: 3693–3702.

Dyke, G., et al. 2013. Aerodynamic performance of the feathered dinosaur *Microraptor* and the evolution of feathered flight. Nature Communications 4: 2489.

Eklund, M.J., A.K. Aase, and C.J. Bell. 2018. Progressive photonics: methods and applications of sequential imaging using visible and non-visible spectra to enhance data-yield and facilitate forensic interpretation of fossils. Journal of Paleontological Techniques 20: 1–36.

Falk, A.R., T.G. Kaye, Z.H. Zhou, and D.A. Burnham. 2016. Laser fluorescence illuminates the soft tissue and life habits of the Early Cretaceous bird *Confuciusornis*. PLoS One 11: e0167284.

Feduccia, A., and H.B. Tordoff. 1979. Feathers of *Archaeopteryx*: asymmetric vanes indicate aerodynamic function. Science 203: 1021–1022.

Feo, T.J., D.J. Field, and R.O. Prum. 2015. Barb geometry of asymmetrical feathers reveals a transitional morphology in the evolution of avian flight. Proceedings of the Royal Society B 282: 20142864.

Field, D.J. 2017. Preliminary paleoecological insights from the Pliocene avifauna of Kanapoi, Kenya: implications for the ecology of *Australopithecus anamensis*. Journal of Human Evolution: in press.

Field, D.J., C. Lynner, C. Brown, and S.A. Darroch. 2013. Skeletal correlates for body mass estimation in modern and fossil flying birds. PLoS One 8: e82000.

Foth, C., H. Tischlinger, and O.W.M. Rauhut. 2014. New specimen of *Archaeopteryx* provides insights into the evolution of pennaceous feathers. Nature 511: 79–82.

Gatesy, S.M. 2001. The evolutionary history of the theropod caudal locomotor module. *In* Gauthier, J., and J.F. Gall (editors), New perspectives on the origin and early evolution of birds: 333–350. New Haven: Peabody Museum of Natural History, Yale University.

Gatesy, S.M., and K.P. Dial. 1996. From frond to fan: *Archaeopteryx* and the evolution of short-tailed birds. Evolution 50: 2037–2048.

George, J.C., and A.J. Berger. 1966. Avian myology, New York: Academic Press.

Gill, F., and D. Donsker (editors). 2017. IOC World Bird List (v 7.3).

Gillooly, J.F., J.H. Brown, G.B. West, V.M. Savage, and E.L. Charnov. 2001. Effects of size and temperature on metabolic rate. Science 293: 2248–2251.

Gillooly, J.F., E.L. Charnov, G.B. West, V.M. Savage, and J.H. Brown. 2002. Effects of size and temperature on developmental time. Nature 417: 70–73.

Greenewalt, C.H. 1975. The flight of birds: the significant dimensions, their departure from the require-

ments for dimensional similarity, and the effect on flight aerodynamics of that departure. Transactions of the American Philosophical Society 65: 1–67.

Guillemette, M., and J.F. Ouellet. 2005. Temporary flightlessness in pre-laying Common Eiders *Somateria mollissima*: are females constrained by excessive wing-loading or by minimal flight muscle ratio? Ibis 147: 293–300.

Hartman, F.A. 1961. Locomotor mechanisms of birds. Smithsonian Miscellaneous Collections 143: 1–91.

Heers, A.M., and R.M. Carney. 2017. Building a bird: a musculoskeletal model of the *Archaeopteryx* flight apparatus. Journal of Vertebrate Paleontology Programs and Abstracts 127.

Heers, A.M., and K.P. Dial. 2012. From extant to extinct: locomotor ontogeny and the evolution of avian flight. Trends in Ecology & Evolution 27: 296–305.

Heers, A.M., B. Tobalske, and K.P. Dial. 2011. Ontogeny of lift and drag production in ground birds. The Journal of Experimental Biology 214: 717–725.

Heers, A.M., D.B. Baier, B.E. Jackson, and K.P. Dial. 2016. Flapping before flight: high resolution, three-dimensional skeletal kinematics of wings and legs during avian development. PLoS One 11: e0153446.

Heers, A.M., J.W. Rankin, and J.R. Hutchinson. 2018. Building a bird: musculoskeletal modeling and simulation of wing-assisted incline running during avian ontogeny. Frontiers in Bioengineering and Biotechnology 6: 140.

Hone, D.W.E., H. Tischlinger, X. Xu, and F.C. Zhang. 2010. The extent of the preserved feathers on the four-winged dinosaur *Microraptor gui* under ultraviolet light. PLoS One 5: e9223.

Hutchinson, J.R. 2011. On the inference of function from structure using biomechanical modelling and simulation of extinct organisms. Biological Letters 8: rsbl.2011.0399.

Hutchinson, J.R., F.C. Anderson, S.S. Blemker, and S.L. Delp. 2005. Analysis of hindlimb muscle moment arms in *Tyrannosaurus rex* using a three-dimensional musculoskeletal computer model: implications for stance, gait, and speed. Paleobiology 31: 676–701.

Jenkins, F.A., Jr. 1993. The evolution of the avian shoulder joint. American Journal of Science 293A: 253–267.

Kaye, T.G., et al. 2015. Laser-stimulated fluorescence in paleontology. PLoS One 10: e0125923.

Kaye, T.G. et al. 2019. Detection of lost calamus challenges identity of isolated *Archaeopteryx* feather. Scientific Reports 9: 1182.

Lefèvre, U., A. Cau, D.Y. Hu, and P. Godefroit. 2020. Feather evolution in Pennaraptora. *In* C. Foth and O.W.M. Rauhut (editors), The evolution of feathers: 67-78. Cham, Switzerland: Springer.

Lentink, D., A.F. Haselsteiner, and R. Ingersoll. 2015. In vivo recording of aerodynamic force with an aerodynamic force platform: from drones to birds. Journal of the Royal Society Interface 12 (104): rsif.2014.1283.

Liu, D., et al. 2017. Flight aerodynamics in enantiornithines: information from a new Chinese Early Cretaceous bird. PLoS One 12: e0184637.

Liu, D., et al. 2019. Soft tissue preservation in two new enantiornithine specimens (Aves) from the Lower Cretaceous Huajiying Formation of Hebei Province, China. Cretaceous Research 95: 191-207.

Livezey, B.C. 1992. Flightlessness in the Galápagos cormorant (*Compsohalieus* [*Nannopterum*] *harrisi*): heterochrony, giantism and specialization. Zoological Journal of the Linnean Society 105: 155–224.

Longrich, N.R., T. Tokaryk, and D.J. Field. 2011. Mass extinction of birds at the Cretaceous–Paleogene (K–Pg) boundary. Proceedings of the National Academy of Sciences of the United States of America 108: 15253–15257.

Louchart, A., et al. 2009. Taphonomic, avian, and small-vertebrate indicators of *Ardipithecus ramidus* habitat. Science 326: 66-66e64.

Manal, K., and T.S. Buchanan. 2004. Subject-specific estimates of tendon slack length: a numerical method. Journal of Applied Biomechanics 20: 195–203.

Marden, J.H. 1987. Maximum lift production during takeoff in flying animals. Journal of Experimental Biology 130: 235–258.

Marden, J.H. 1994. From damselflies to pterosaurs: how burst and sustainable flight performance scale with size. American Journal of Physiology-Regulatory Integrative and Comparative Physiology 35: R1077–R1084.

Meseguer, J., and A. Sanz-Andres. 2007. Aerodinamica del vuelo: Aves y Aeronaves. Madrid: Aeropuertos Españoles y Navegacion Aerea.

Meunier, K. 1951. Korrelation und umkonstruktion in den grössenbeziehungen zwischen vogelflügel und vogelkörper (Correlation and restructuring in the size relationship between avian wing and avian body). Biologia Generalis 19: 403–443.

Navalón, G., J. Marugán-Lobón, L.M. Chiappe, J.L. Sanz, and Á.D. Buscalioni. 2015. Soft-tissue and dermal arrangement in the wing of an Early Cretaceous bird: Implications for the evolution of avian flight. Scientific Reports 5: 14864.

Navalón, G., et al. 2018. Diversity and evolution of Confuciusornithidae: evidence from a new 131-million-

year-old specimen from the Huajiying Formation in NE China. Journal of Asian Earth Sciences 152: 12–22.

Norberg, U.M. 2002. Structure, form, and function of flight in engineering and the living world. Journal of Morphology 252: 52–81.

Nudds, R.L., and G.J. Dyke. 2010. Narrow primary feather rachises in *Confuciusornis* and *Archaeopteryx* suggest poor flight ability. Science 328: 886–889.

O'Neill, M.C., et al. 2013. A three-dimensional musculoskeletal model of the chimpanzee (*Pan troglodytes*) pelvis and hind limb. Journal of Experimental Biology 216: 3709–3723.

Otero, A., V. Allen, D. Pol, and J.R. Hutchinson. 2017. Forelimb muscle and joint actions in Archosauria: insights from *Crocodylus johnstoni* (Pseudosuchia) and *Mussaurus patagonicus* (Sauropodomorpha). PeerJ 5: e3976.

Pei, R., et al. In press. Potential for powered flight neared by most close avialan relatives but few crossed its thresholds. Current Biology.

Pennycuick, C.J. 2008. Modelling the flying bird, London: Academic Press.

Pittman, M., S.M. Gatesy, P. Upchurch, A. Goswami, and J.R. Hutchinson. 2013. Shake a tail feather: the evolution of the theropod tail into a stiff aerodynamic surface. PLoS One 8: e63115.

Pollock, C.M., and R.E. Shadwick. 1994. Relationship between body mass and biomechanical properties of limb tendons in adult mammals. American Journal of Physiology-Regulatory, Integrative and Comparative Physiology 266: R1016–R1021.

Poore, S.O., A. Ashcroft, A. Sánchez-Haiman, and G.E. Goslow. 1997a. The contractile properties of the M. supracoracoideus in the pigeon and starling: a case for long-axis rotation of the humerus. Journal of Experimental Biology 200: 2987–3002.

Poore, S.O., A. Sánchez-Haiman, and G.E. Goslow Jr. 1997b. Wing upstroke and the evolution of flapping flight. Nature 387: 799–802.

Prum, R.O., et al. 2015. A comprehensive phylogeny of birds (Aves) using targeted next-generation DNA sequencing. Nature 526: 569–573.

Rauhut, O.W.M., C. Foth, and H. Tischlinger. 2018. The oldest *Archaeopteryx* (Theropoda: Avialiae): a new specimen from the Kimmeridgian/Tithonian boundary of Schamhaupten, Bavaria. PeerJ 6: e4191.

Rayner, J.M. 1988. The evolution of vertebrate flight. Biological Journal of the Linnean Society 34: 269–287.

Rayner, J.M. 1993. On aerodynamics and the energetics of vertebrate flapping flight. Contemporary mathematics 141: 351–400.

Rosset, A., L. Spadola, and O. Ratib. 2004. OsiriX: an open-source software for navigating in multidimensional DICOM images. Journal of Digital Imaging 17: 205–216.

Rowe, T., et al. 2001. Forensic palaeontology: the *Archaeoraptor* forgery. Nature 410(6828): 539–540.

Schilling, R., B. Jastram, O. Wings, D. Schwarz-Wings, and A.S. Issever. 2014. Reviving the dinosaur: virtual reconstruction and three-dimensional printing of a dinosaur vertebra. Radiology 270: 864–871.

Schmidt-Nielsen, K. 1984. Scaling: why is animal size so important? Cambridge: Cambridge University Press.

Serrano, F.J., and L.M. Chiappe. 2017. Aerodynamic modelling of a Cretaceous bird reveals thermal soaring during avian evolution. Journal of the Royal Society Interface 14: 20170182.

Serrano, F.J., P. Palmqvist, and J.L. Sanz. 2015. Multivariate analysis of neognath skeletal measurements: implications for bodymass estimation in Mesozoic birds. Zoological Journal of the Linnean Society 173: 929–955.

Serrano, F.J., P. Palmqvist, L.M. Chiappe, and J.L. Sanz. 2017. Inferring flight parameters of Mesozoic avians through multivariate analyses of forelimb elements in their living relatives. Palaeobiology 43: 144–169.

Serrano, F.J., et al. 2018. Flight reconstruction of two European enantiornithines (Aves, Pygostylia) and the achievement of bounding flight in Early Cretaceous birds. Palaeontology 61: 359–368.

Shyy, W., Y.S. Lian, J. Tang, D. Viieru, and H. Liu. 2008. Aerodynamics of low Reynolds number flyers. Cambridge: Cambridge University Press.

Smith, N.D. 2012. Body mass and foraging ecology predict evolutionary patterns of skeletal pneumaticity in the diverse "waterbird" clade. Evolution 66: 1059–1078.

Swaddle, J.P., and R. Lockwood. 2003. Wingtip shape and flight performance in the European Starling *Sturnus vulgaris*. Ibis 145: 457–464.

Tennekes, H. 2009. The simple science of flight: from insects to jumbo jets, Cambridge: MIT Press.

Tischlinger, H., and D. Unwin. 2004. UV-Untersuchungen des Berliner Exemplars von *Archaeopteryx lithographica* H. v. Meyer 1861 und der isolierten *Archaeopteryx*-Feder. *Archaeopteryx* 22: 17–50.

Tobalske, B.W., and A.A. Biewener. 2008. Contractile properties of the pigeon supracoracoideus during different modes of flight. Journal of Experimental Biology 211: 170–179.

Tobalske, B.W., and K.P. Dial. 2007. Aerodynamics of wing-assisted incline running in birds. Journal of Experimental Biology 210: 1742–1751.

van Oorschot, K.B., H.K. Tang, and B.W. Tobalske. 2017. Phylogenetics and ecomorphology of emarginate primary feathers. Journal of Morphology 278: 936–947.

Videler, J.J. 2005. Avian flight. Oxford: Oxford University Press.

Von Mises, R. 1945. Theory of flight. *In* 672. New York: Dover Publications.

Wang, X.L., et al. 2017. Basal paravian functional anatomy illuminated by high-detail body outline. Nature Communications 8: 14576.

Wellnhofer, P. 2009. *Archaeopteryx* – the icon of evolution, München: Verlag Dr. Friedrich Pfeil.

Xu, X. 2020. Filamentous integuments in nonavialan theropods and their kin: advances and future perspectives for understanding the evolution of feathers. *In* C. Foth and O.W.M. Rauhut (editors), The evolution of feathers: 67–78. Cham, Switzerland: Springer.

Xu, X., et al. 2003. Four-winged dinosaurs from China. Nature 421: 335–340

Xu, X., et al. 2015. A bizarre Jurassic maniraptoran theropod with preserved evidence of membranous wings. Nature 521: 70–73.

Zajac, F.E. 1989. Muscle and tendon: properties, models, scaling, and application to biomechanics and motor control. Critical Reviews in Biomedical Engineering 17: 359–411.

Zheng, X.T., et al. 2014. On the absence of sternal elements in *Anchiornis* (Paraves) and *Sapeornis* (Aves) and the complex early evolution of the avian sternum. Proceedings of the National Academy of Sciences of the United States of America111: 13900–13905.

Zhou, Z.H., and F.C. Zhang. 2002. A long-tailed, seed-eating bird from the Early Cretaceous of China. Nature 418: 405–409.